Structure transition, formation, and optical absorption property study of Ag/SiO_2 nanofilm by sol–gel method

Yan Li and Bo-Ping Zhang[a)]
School of Materials Science and Engineering, University of Science and Technology Beijing, Beijing 100083, China

Cui-Hua Zhao
College of Materials Science and Engineering, Guangxi University, Nanning 530004, China

Jin-Xian Zhao
School of Materials Science and Engineering, University of Science and Technology Beijing, Beijing 100083, China

(Received 30 May 2012; accepted 22 October 2012)

Ag nanoparticles dispersed SiO_2 composite films were successfully prepared by a sol–gel method. The structural transition, formation, and optical property along with relevant band gap of Ag/SiO_2 thin films during the annealing process were studied by Fourier transform infrared spectroscopy, thermogravimetry–differential thermal analysis, x-ray diffraction, and ultraviolet–visible spectroscopy, while the microstructure of thin films was revealed by transmission electron microscopy. The results indicate that the Ag spherical particles with the diameter of 10–20 nm were formed by breaking Si–O–Ag bonds above 200 °C and dispersed in the SiO_2 matrix. The optical absorption property of Ag/SiO_2 nanofilm in the visible range is enhanced, and the band gap (E_g) is widened with raising annealing temperatures, which is promising for the potential applications in nonlinear optical and related fields.

I. INTRODUCTION

Metal nanoparticle (NP) dispersed nanooxide films have attracted much attention for decades due to their enhanced nonlinear optical properties benefiting the fundamental studies and practical applications. The enhanced nonlinear optical properties are induced from the surface plasmon of resonance (SPR) of metal particles, and the optical absorption peak can be controlled in the visible range by adjusting the content, size, and shape of the particles.[1,2] Specially, silver NPs dispersed silica dioxide (Ag/SiO_2) nanocomposite, which exhibit enhanced nonlinear optical properties in the visible range, have inspired growing interest on account of their potential applications in nonlinear optics,[3,4] photonic devices,[5,6] and fluorescence enhancement.[7] Nowadays, the methods available to prepare Ag/SiO_2 composite film include chemical approach,[6] ion beam mixing process,[8] ion implantation,[9] magnetron sputtering,[10,11] and sol–gel method.[12,13] Among them, magnetron sputtering and ion implantation techniques can easily yield high-quality film but need high cost and vacuum conditions for preparation, as well as difficult to control component radio of the composite film and retain high mental content. Although chemical approach can easy to form Ag/SiO_2 composite film with low cost, it is also hard to realize high mental content, which limits their optical absorption properties further enhancing. Sol–gel technique is one of the most common methods and provides many advantages over other methods because of their low formation temperature, high degree of homogeneity, high yield, small processing time, possibility of coating on large area substrates, easy to control component radio of the composite film, cost-effective, and environment friendly.[12–14] Therefore, sol–gel technique is widely used in preparing Ag/SiO_2 composite film. However, to the best of our knowledge, the forming mechanism of the Ag NPs dispersed SiO_2 composite films prepared by sol–gel method has received less investigation. In this study, the structural transition, the formation, and the optical absorption property along with the relevant band gap of the Ag/SiO_2 thin films obtained by sol–gel method during the annealing process were investigated.

II. EXPERIMENTAL

The Ag/SiO_2 composite thin film with 50 wt% Ag was prepared by a sol–gel spin-coating method. Tetraethyl orthosilicate [$Si(OC_2H_5)_4$] and silver nitrate ($AgNO_3$) were used as raw materials and 2-ethoxyethanol ($CH_3OCH_2CH_2OH$) as a solvent. The concentration of precursor solutions was controlled at 0.445 mol/L. Volume ratio of $CH_3OCH_2CH_2OH$ to water was 1:8. $Si(OC_2H_5)_4$, $CH_3OCH_2CH_2OH$, and distilled water were mixed and stirred for 7 h at room temperature. Several drops of nitric acid were added before stirring as hydrolysis catalysis for adjusting the pH value of solution between 2 and 3. After

a)Address all correspondence to this author.
e-mail: bpzhang@ustb.edu.cn
DOI: 10.1557/jmr.2012.388

 © Materials Research Society 2012

https://doi.org/10.1557/jmr.2012.388 Published online by Cambridge University Press

dissolving silver nitrate in the above solution with a weight ratio of $Ag/(Ag + SiO_2) = 50$ wt%, the solution was further stirred for 5 h. A transparent and colorless Ag/SiO_2 precursor solution was obtained.

The Ag/SiO_2 nanofilms were spin coated on a glass substrate at a spin speed of 3000 rpm. After each coating, the precursor film was preheated at 150 °C for 30 s to remove the solvent and a small amount of water. Then, these sequences of coating and pretreatment were repeated 2 times for the absorption measurement and 10 times for the x-ray diffraction (XRD) analysis, respectively. The annealing temperature of Ag/SiO_2 nanofilms was carried out in the range from 200 to 600 °C for 30 min.

The thermal analysis was performed on the gel-dried powders using thermogravimetry–differential thermal analysis (TG–DTA; HCT-1, Beijing Optical Instrument Inc., China) analyzer with a heating rate of 10 °C/min. The crystal structure was analyzed using x-ray powder diffraction with a Cu K_α radiation ($\lambda = 0.15406$ nm) filtered through a Ni foil (RAD-B system; Rigaku, Tokyo, Japan). The average size of Au particle was calculated using the (111) reflection by the Scherrer equation $D = K\lambda/\beta\cos\theta$, where D is the average particle size, K the Scherrer constant 0.89, λ the x-ray wave length 0.154 nm, and β the full width at half maximum (FWHM) of the XRD peak. The microstructure was observed by transmission electron microscopy (TEM; JEM-100CXΠ, JEOL, Tokyo, Japan). Fourier transform infrared (FTIR) transmission spectra were recorded using a FTIR spectrometer. Ultraviolet–visible absorption spectra of the films were measured in the range of 350–800 nm using a UV2800 spectrophotometer (UNICO Instruments Co., Ltd., China).

III. RESULTS

Figure 1 shows the DTA and TG curves of pure SiO_2 and Ag/SiO_2 powders, which were prepared by drying the precursor solution at 60 °C in air for a week. For the pure SiO_2 powder sample, the weight loss occurs at three stages: namely, (i) below 200 °C, (ii) between 200 and 350 °C, and (iii) from 350 to 600 °C. Evidently, DTA curve corresponds to that of TGA, i.e., the two endothermic peaks and three exothermic peaks are just in the range of the significant weight loss, which is between 200 and 350 °C and from 350 to 600 °C. The big endothermic peak at 78 °C and the weak endothermic peak at 177.8 °C corresponding to a weight loss of 15% are due to the evaporation of both water and ethanol, which come from the hydrolysis and condensation reactions of $Si(OC_2H_5)_4$ as indicated in the reactions [Eqs. (1) and (2)][15]:

$$Si(OC_2H_5)_4 + H_2O \rightarrow (OC_2H_5)_3Si - OH + C_2H_5OH \quad , \tag{1}$$

$$(C_2H_5O)_3Si - OH + HO - Si(OC_2H_5)_3 \rightarrow (C_2H_5O)_3Si - O - Si(OC_2H_5)_3 + H_2O \quad . \tag{2}$$

The exothermic peak at 345 °C is attributed to the pyrolysis of the residual oxyethyl groups ($-OC_2H_5$).[16] And the peaks at 413 and 455 °C may be ascribed to the combustion of residual carbon in the matrix and organic compounds.[17,18] While in this process, SiO_2 was finally obtained after decomposition reaction of $Si_nO_n(OH)_{4-n}$, which was formed through the dehydration and condensation reactions after the $-OH$ replaced the $-C_2H_5O$ group of $(C_2H_5O)_3Si–O–Si(OC_2H_5)_3$. Such reaction may continue until 700 °C since the weight loss ended till this temperature. However, for the Ag/SiO_2 powder sample, a similar trace below 200 °C and an obvious difference over 200 °C are observed in Fig. 1 compared with the SiO_2 powder sample. The three exothermic peaks at 203, 250, and 280 °C, respectively, indicate that the pyrolysis reaction and removal of residual organic compounds were accelerated by adding $AgNO_3$ into the SiO_2 precursor solution. However, no peaks around 440 °C resulting from the decomposition of silver nitrate were detected,[9] indicating that the $Si(OC_2H_5)_4$ and silver nitrate should react below 345 °C, which will be discussed later.

Figure 2 shows XRD patterns of the as-deposited Ag/SiO_2 thin film and the annealed counterparts. A broad diffraction peak at 25° for all the samples corresponds to the amorphous SiO_2 matrix and/or the glass substrate.[19] No diffraction peaks of Ag crystal appear in the as-deposited sample. When the thin film was annealed at 300 °C, three diffraction peaks are observed at 38.1°, 44.4°, and 64.6°, which attribute to the Ag (111), (200), and (220) planes, respectively, demonstrating the formation of Ag particles in SiO_2 matrix. Furthermore, those three diffraction peaks intensify with raising annealing temperature from 300 to 500 °C, suggesting the improvement of crystalline Ag particles. Besides, the mean sizes of the Ag particles calculated

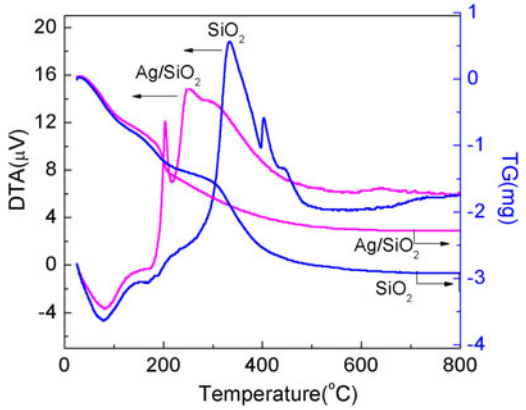


FIG. 1. DTA–TG curve of gel powders for the pure SiO_2 and Ag/SiO_2.

https://doi.org/10.1557/jmr.2012.388 Published online by Cambridge University Press

by the Scherrer equation increase from 10 to 20 nm as the annealing temperature raises from 300 to 500 °C.

Figure 3(a) shows the bright field TEM micrograph and the corresponding selective area electron diffraction pattern of Ag/SiO_2 thin film annealed at 500 °C. As shown in the inset of Fig. 3(a), the diffraction rings from inner to outer correspond to Ag crystal faces (111), (200), (220), (311), and (222) of Ag/SiO_2 thin film, respectively, which coincide well with that of the XRD analysis. The bright field TEM micrograph indicates that Ag particles are basically spherical and dispersed in the SiO_2 matrix. Figure 3(b) shows the corresponding particle size distribution histogram of the Ag particles. As can be seen that the size of Ag particles is in the range of 10–40 nm, and the maximum size is 40 nm. However, according to our calculation by the method of Soderlund et al.,[20] the distribution does not obey lognormal distribution function, maybe resulting from the different growth mechanism.

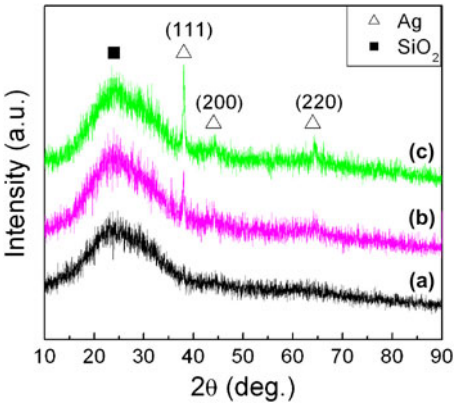


FIG. 2. XRD patterns of as-deposited (a) Ag/SiO_2 thin film and the annealed counterparts at 300 °C (b) and 500 °C (c).

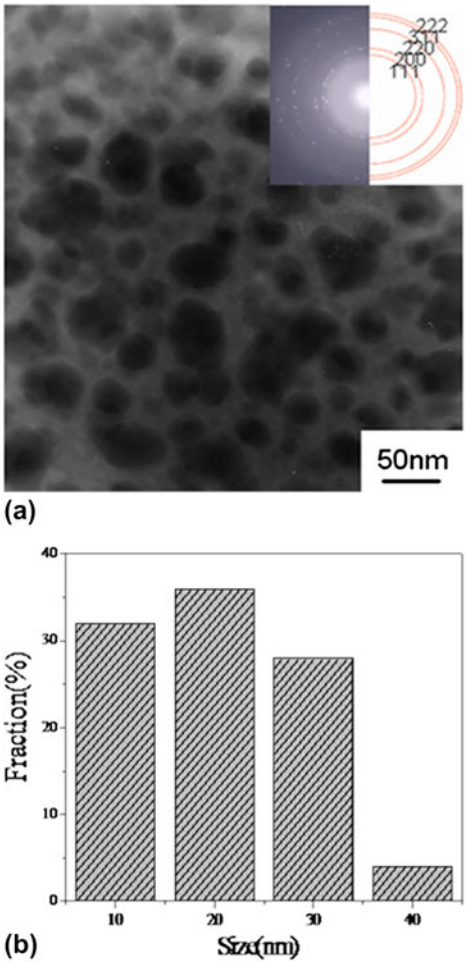


FIG. 3. (a) TEM micrograph and the selected area electron diffraction patterns of Ag/SiO_2 thin film annealed at 500 °C. (b) The particle size distribution histogram of the sample corresponding to (a).

FTIR transmission spectra of the as-deposited Ag/SiO_2 film, the corresponding samples, which were annealed at 300 °C (c) and 500 °C (d), respectively, and the as-deposited pure SiO_2 are included in Fig. 4 for comparison. For the pure SiO_2 sample, there are eight absorption peaks at 1077, 796, and 449 cm^{-1} for Si–O–Si bonds,[21–23] at 945 and 571 cm^{-1} for Si–OH bonds,[15,24] at around 1200 cm^{-1} for Si–OC_2H_5 bands,[25] at 1385 cm^{-1} for O–N–O bands,[19] and at 1639 cm^{-1} for H–O–H bound,[17] respectively. The Si–O–Si band centered at 449 cm^{-1} is assigned to transverse–optical rocking motions, and the Si–O–Si band centered at 796 cm^{-1} is due to transverse–optical symmetric stretching of the O atom. The highest frequency band near 1077 cm^{-1} with the highest intensity is associated with the asymmetrical O–Si–O stretch motion in which adjacent O atoms move in phase with each other.[26,27] The Si–OH vibrations detected at 571 and 945 cm^{-1} are probably due to silanol groups. The Si–OC_2H_5 band around 1200 cm^{-1} can be assigned to the incomplete hydrolysis of $Si(OC_2H_5)_4$. The O–N–O band at 1385 cm^{-1} is attributed to NO_3^- ions. The band of 1639 cm^{-1} is due to the H–O–H deformation, which indicates the presence of water incorporated in the silica matrix.[17] The assignments and the wave number values of the bands observed for all the samples are listed in Table I.

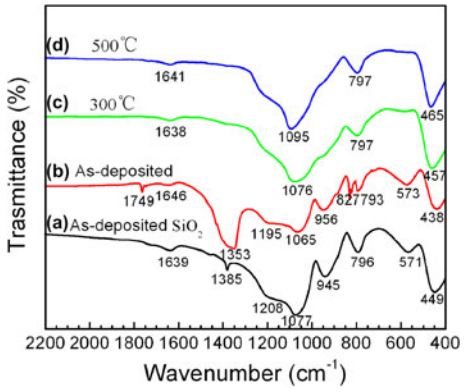


FIG. 4. FTIR spectra of the as-deposited SiO_2 thin film (a) as well as the as-deposited Ag/SiO_2 thin films (b) and their annealed samples at 300 °C (c) and 500 °C (d).

https://doi.org/10.1557/jmr.2012.388 Published online by Cambridge University Press

When silver nitrate was added to the $Si(OC_2H_5)_4$ precursor solution, all Si–O–Si bands shift to lower wave number from 1077, 796, and 449 cm^{-1} to 1065, 793, and 438 cm^{-1}, respectively, along with a decreased intensity as shown in Fig. 4(b). The decreased wave numbers imply a reduction in the vibrational energy,[28] and the weakened original silica gel network may be attributed to the addition of silver nitrate. However, both Si–OH stretching bands shift to higher wave number from 945 and 571 cm^{-1} to 956 and 573 cm^{-1}, and the intensity of the 945 cm^{-1} peak becomes weaker. A fact is that the frequency position of Si–OH bands is related to the degree of hydrogen bonding in the film; therefore, the peak shift to a high wave number could be attributed to an increase in the Si–OH force constant.[29] And the O–N–O band at 1385 cm^{-1} is intensified because of the adding of NO_3^-. Besides those, a special feature for the Ag/SiO_2 sample is the appearance of new absorption peaks at 827 and 1749 cm^{-1}, which are considered as the Si–O–Ag bond vibrations and a hydrophilic silica xerogel structure that can form by absorbing water from air, respectively.

When the Ag/SiO_2 film was annealed at 300 and 500 °C, the Si–O–Ag band at 827 cm^{-1}, two Si–OH bands at 945 and 571 cm^{-1}, and O–N–O band at 1385 cm^{-1} along with absorption band at 1749 cm^{-1} disappear as shown in Figs. 4(c) and 4(d). All the Si–O–Si bands intensified and shift to higher wave number, to 1076, 797, and 457 cm^{-1} for the 300 °C annealed sample and to 1095, 797, and 465 cm^{-1} for the 500 °C annealed sample. This shift reflects an increased rigidity of the Si–O–Si network during the condensation process, and the increased intensity is due to the intensified structural disorder of SiO_2 thin film by raising temperature.[30–32] However, the FWHM of the peak narrows when the annealing temperature increases from 300 to 500 °C, which may be due to the densification of the film as the stretching of Si–O–Si bond at 500 °C is less than that one at 300 °C. The decreased intensity of the Si–OC_2H_5 with increasing temperature from 0 to 500 °C may be attributed to the partial decomposition of Si–OC_2H_5 into Si–OH. The band intensity of 1639 cm^{-1} owing to the bending of the absorbed water molecules decreases with increasing temperature because of the removal of water. The disappearance of O–N–O band after annealing above 300 °C reveals the formation of the nitrogen oxide gases in acidic SiO_2 sol.[21] The dehydration of the hydrophilic silica xerogel structure by annealing induces the absence of the band at 1749 cm^{-1}.

Figure 5 shows the optical absorption spectra of Ag/SiO_2 thin film, which were annealed at different temperatures. All the samples exhibit an obviously enhanced optical absorption property at 420 nm due to the SPR effect of Ag nanoparticles (NPs) except for the sample annealed at 200 °C, which reveals that Ag particles were formed above 200 °C. This fact is also in well agreement with the results of DTA curve (Fig. 1) and XRD pattern (Fig. 2). The samples annealed at 300 °C showed a broader absorption peak with a low intensity while exhibited an intensified absorption peak with a narrowed bandwidth along with a blueshift trend as the annealing temperature was increased to 500 and 600 °C. For further understanding the behavior of the optical absorption, the energy band gap (E_g) was estimated by the method of Zhao et al.[33] (Fig. 6). The dependence of $(\alpha h\upsilon)^2$ in Fig. 6 as a function of

TABLE I. Vibrational bands assignment and wave number (cm^{-1}) of the as-deposited SiO_2, as-deposited, and annealed Ag/SiO_2 at 300 and 500 °C.

	Wave number (cm^{-1})			
		Ag/SiO_2		
Assignment	As-deposited SiO_2	As-deposited	Annealed at 300 °C	Annealed at 500 °C
υ_{as}(Si–O–Si)	1077	1065	1076	1095
υ_s(Si–O–Si)	796	793	797	797
δ(Si–O–Si)	449	438	457	465
υ(Si–OH)	945	956	...	...
υ(Si–OH)	571	573	...	...
$\upsilon(NO^{3-})$	1385	1353	...	...
υ(Si–OC_2H_5)	1208	1195	...	...
$\delta(H_2O)$	1639	1646	1638	1641
$\upsilon(H_2O)$	...	1749	...	...

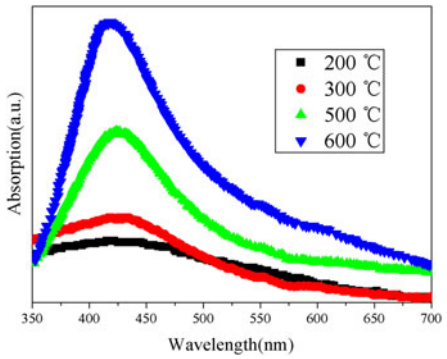


FIG. 5. Optical absorption spectra for the Ag/SiO_2 thin films annealed at different annealing temperatures.

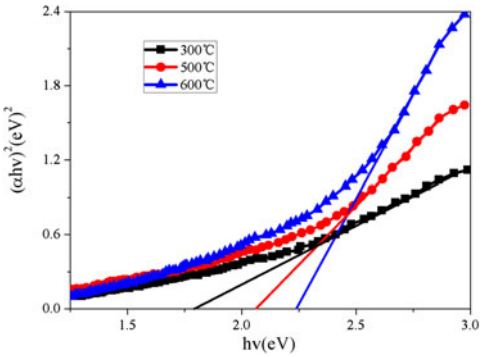


FIG. 6. Relationship between $(\alpha h\upsilon)^2$ and $h\upsilon$ for Ag/SiO_2 thin film.

https://doi.org/10.1557/jmr.2012.388 Published online by Cambridge University Press

photon energy *hv* indicates that all samples are the directly allowed nature of band-to-band transitions. The E_g in the plot of $(\alpha h\upsilon)^2$ and *hv* is 1.80, 2.05, and 2.23 eV for the Ag/SiO_2 nanocomposite films annealed at 300, 500, and 600 °C, respectively. The E_g is gradually widened with increasing the annealing temperature as a result of blueshift of the SPR peaks, which is in agreement with the optical absorption spectra survey mentioned above.

IV. DISCUSSION

The Ag NPs in the SiO_2 film not only affect the optical properties (Fig. 5) of the Ag/SiO_2 thin films but also change the xerogel structure (Figs. 1 and 4). In the pure SiO_2 xerogel, the condensation reaction (2) of silicate groups usually occurs initially at room temperature and accelerated with increasing temperature from room temperature to 177.8 °C.[34] When $AgNO_3$ was added in the sol, the vibrational absorption peak of the Si–O–Ag bond appears at 827 cm^{-1} in the as-prepared Ag/SiO_2 film as shown in Fig. 4(b). This result indicates that except for the reaction (2), the reaction (3) for the formation of $(C_2H_5O)_3Si$–O–Ag compound as indicated in the following should occur at room temperature[35]:

$$(C_2H_5O)_3Si - O - H + Ag^+ = (C_2H_5O)_3Si - O - Ag + H^+ \quad . \tag{3}$$

As the reaction (3) processes, the number of Si–OH band (956 cm^{-1}) taken in reaction (2) should decrease, resulting in all the Si–O–Si bands weaken at about 1076–1095, 793–797, and 438–465 cm^{-1} of the as-prepared Ag/SiO_2 film. However, the peak at 827 cm^{-1} of Si–O–Ag band disappears after annealing at 300 and 500 °C as shown in Figs. 4(b)–4(d), indicating that the Si–O–Ag bonds can decompose completely at 300 °C, while $AgNO_3$ usually decomposes over 440 °C. Hence, the appeared exothermal peak in the Ag/SiO_2 powder at 203 °C in Fig. 1 can be attributed to the decomposition of Si–O–Ag into the metal Ag particles. Furthermore, XRD analyses in Fig. 2 and the optical absorption spectrum also confirm that Ag particles were formed below 300 °C. On the one hand, when the Ag/SiO_2 film was annealed at 300 and 500 °C, the peaks at 945 and 571 cm^{-1} of Si–OH bands disappear in Figs. 4(c) and 4(d), suggesting the end of the reactions (3) and (2). As a result, the Si–O–Si bands at about 1076–1095, 793–797, and 438–465 cm^{-1}(Fig. 4) intensify with increasing temperature. On the other hand, when the annealing was carried out on the Ag/SiO_2 film below 200 °C, no essential absorption in the visible region of spectrum was observed given by the absence of the metal Ag particles because $(C_2H_5O)_3Si$–O–Ag compound begins to decompose at about 203 °C (Fig. 1). A relatively weaker absorption peak appears in the sample annealed at 300 °C due to the incomplete decompose of $(C_2H_5O)_3Si$–O–Ag compound (Fig. 5).

V. CONCLUSIONS

Ag/SiO_2 nanocomposite films were prepared by a sol–gel method. The FTIR transmission spectra and DTA–TG curve exhibited that the Si–O–Ag bonds formed at room temperature by the interaction between $(OC_2H_5)_3Si$–OH and $AgNO_3$ and then decomposed into Ag particle at above 200 °C. XRD results and TEM micrograph confirmed that the spherical Ag particles with 10–20 nm in diameter were dispersed in the Ag/SiO_2 nanofilms after annealing at 300 °C and above 300 °C. The enhanced optical absorption property with increasing the annealing temperature over 200 °C is due to the formation and the growth of the Ag particles, whereas the high dispersion of Ag particles results in the blueshift of the SPR peaks and E_g with increasing the annealing temperature.

ACKNOWLEDGMENTS

The authors thank Mr. Xi-Zhen Ding (graduate student of USTB) for a part of his experiments. This work was supported by Major State Basic Research Development (Grant No. 2007CB613301), the National Natural Science Foundation of China (Grant No. 50972012), and Specialized Research Fund for the Doctoral Program of Higher Education (Grant No. 20090006110010).

REFERENCES

1. U. Kreibig and M. Vollmer, *Optical Properties of Metal Clusters* (Springer-Verlag, Berlin, Germany, 1995).
2. C. Sella, S. Chenot, V. Reillon, and S. Berthier: Influence of the deposition conditions on the optical absorption of Ag-SiO2 nanocermet thin films. *Thin Solid Films* **517**, 5848 (2009).
3. U. Kreibig and L. Genzel: Optical absorption of small metallic particles. *Surf. Sci.* **156**, 678 (1985).
4. B.J. Persson: Surface resistivity and vibrational damping in adsorbed layers. *Phys. Rev. B* **44**, 3277 (1991).
5. G.D. Stucky and J.E. Mac Dougall: Quantum confinement and host/guest chemistry: Probing a new dimension. *Science* **247**(4943), 669 (1990).
6. A.A. Scalisi, G. Compagnini, L. D'Urso, and O. Puglisi: Nonlinear optical activity in Ag-SiO_2 nanocomposite thin films with different silver concentration. *Appl. Surf. Sci.* **226**, 237 (2004).
7. L. Guo, A. Guan, X. Lin, C. Zhang, and G. Chen: Preparation of a new core-shell Ag@SiO_2 nanocomposite and its application for fluorescence enhancement. *Talanta* **82**, 1696 (2010).
8. P. Gangopadhyay, R. Kesavamoorthy, K.G.M. Nair, and R. Dhandapani: Raman scattering studies on silver nanoclusters in a silica matrix formed by ion-beam mixing. *J. Appl. Phys.* **88**(9), 4975 (2000).
9. Z.X. Liu, H. Li, X.D. Feng, S.G. Ren, and H.H. Wang: Formation effects and optical absorption of Ag nanocrystals embedded in single crystal SiO_2 by implantation. *J. Appl. Phys.* **84**(4), 1913 (1998).
10. L. Yang, Y.L. Liu, Q.M. Wang, H.Z. Shi, G.H. Li, and L.D. Zhang: The plasmon resonance absorption of Ag/SiO_2 nanocomposite films. *Microelectron. Eng.* **66**, 192 (2003).
11. I. Tanahashi, M. Yoshida, Y. Manabe, and T. Tohda: Effects of heat treatment on Ag particle growth and optical properties in Ag/SiO_2 glass composite thin films. *J. Mater. Res.* **10**, 362 (1995).

https://doi.org/10.1557/jmr.2012.388 Published online by Cambridge University Press

12. A. Babapour, O. Akhavan, A.Z. Moshfegh, and A.A. Hosseini: Size variation and optical absorption of sol-gel Ag nanoparticles doped SiO_2 thin film. *Thin Solid Films* **515**, 771 (2006).
13. L.S. Jiao, B.P. Zhang, X.Z. Ding, C. Chen, and H.L. Zhang: Sol-gel preparation of Ag/SiO_2 nano-composite films and their optical absorption properties. *Rare Met. Mater. Eng.* **36**, 882 (2007).
14. M. Chatterjee and M.K. Naskar: Sol-gel synthesis of lithium aluminum silicate powders: The effect of silica source. *Ceram. Int.* **32**, 623 (2006).
15. E. Monsivais-Gámez, F. Ruiz, and J.R. Martínez: Four-membered rings family in the Si–O extended rocking IR band from quantum chemistry calculations. *J. Sol-Gel Sci. Technol.* **43**(1), 65 (2007).
16. V.K. Parashar, V. Raman, and O.P. Bahl: The role of N,N, dimethylformamide and glycol in the preparation and properties of sol-gel derived silica. *J. Mater. Sci. Lett.* **15**(16), 1403 (1996).
17. M. Stefanescu, M. Stoia, and O. Stefanescu: Thermal and FT-IR study of the hybrid ethylene-glycol–silica matrix. *J. Sol-Gel Sci. Technol.* **41**(1), 71 (2007).
18. W.X. Que, Y. Zhou, Y.L. Lam, Y.C. Chan, H.T. Tan, T.H. Tan, and C.H. Kam: Sol-gel processed silica/titania/y-glycidoxypropy-ltrimethoxysilane composite materials for photonic applications. *J. Electron. Mater.* **29**(8), 1052 (2000).
19. N.B. Colthup, L.H. Daly, and S.E. Wiberiey: *Introduction to Infrared and Raman Spectroscopy*, 2nd ed (Academic Press, New York, 1975).
20. J. Soderlund, L.B. Kiss, G.A. Niklasson, and C.G. Granqvist: Lognormal size distributions in particle growth processes without coagulation. *Phys. Rev. Lett.* **80**(11), 2386 (1998).
21. B. Karmakar, G. De, and D. Ganguli: Dense silica microspheres from organic and inorganic acid hydrolysis of TEOS. *J. Non-Cryst. Solids* **272**(40239), 119 (2000).
22. G. De, B. Karmakar, and D. Ganguli: Hydrolysis-condensation reactions of TEOS in presence of acetic acid leading to the generation of glass-like silica microspheres in solution at room temperature. *J. Mater. Chem.* **10**, 2289 (2000).
23. G. De, D. Kundu, B. Karmakar, and D. Ganguli: FTIR studies of gel to glass conversion in TEOS-fumed silica derived gels, *J. Non-Cryst. Solids* **155**, 253 (1993).
24. H.J. Jeon, S.C. Yi, and S.G. Oh: Preparation and antibacterial effects of Ag-SiO_2 thin films by sol-gel method. *Biomaterials* **24**, 4921 (2003).
25. J. Wang, C.R. Zhang, and J. Feng: Modification of nanoporous silica film by trimethylchlorosilane. *Acta Phys. Chim. Sin.* **20**, 1399 (2004).
26. P. Innocenzi: Infrared spectroscopy of sol-gel derived silica-based films: A spectra-microstructure overview. *J. Non-Cryst. Solids* **316**(2–3), 309 (2003).
27. J.R. Martinez, F. Ruiz, Y.V. Vorobiev, F. Pérez-Robles, and J. González-Hernández: Infrared spectroscopy analysis of the local atomic structure in silica prepared by sol-gel. *J. Chem. Phys.* **109**(17), 7511 (1998).
28. M. Parler Caroline, A. Ritter James, and D. Amiridis Michael: Infrared spectroscopic study of sol-gel derived mixed-metal oxides, *J. Non-Cryst. Solids* **279**(2–3), 119 (2001).
29. D. Niznansky and J.L. Rehspringer: Infrared study of SiO_2 sol to gel evolution and gel aging. *J. Non-Cryst. Solids* **180**, 191 (1995).
30. M. Yamane: in *Sol-Gel Technology for Thin Films*, edited by L.C. Klein (Noyes Publications, New Jersey, 1989).
31. C.C. Perry, X. Li, and D.N. Waters: Structural studies of gel phases. 4. An infrared reflectance and Fourier-transform Raman-study of silica and silica titania gel glasses. *Spectrochim. Acta* **47**, 1487 (1991).
32. L. Lan, G. Gnappi, and A. Montenero: Infrared study of EPOXS-TEOS-TPOT gels. *J. Mater. Sci.* **28**, 2119 (1993).
33. C.H. Zhao, B.P. Zhang, and P.P. Shang: Enhanced nonlinear optical absorption of Au/SiO_2 nano composite thin films. *Chin. Phys. B* **18**, 5539 (2009).
34. R. Pięknoś, M. Wesołowski, and J. Teodorczyk: Thermal analysis of some pharmaceutically relevant systems obtained by sol-gel technique. *J. Therm. Anal. Calorim.* **70**, 447 (2002).
35. L.H. Allen and E. Matijevic: Stability of colloidal silica: III. Effect of hydrolyzable cations. *Interface Sci.* **35**, 66 (1971).

https://doi.org/10.1557/jmr.2012.388 Published online by Cambridge University Press